Journal of Materials and Environmental Science
ISSN : 2028-2508
e-ISSN : 2737-890X
CODEN : JMESCN

J. Mater. Environ. Sci., 2023, Volume 14, Issue 03, Page 326-336

http://www.jmaterenvironsci.com

Discovery of new inhibitors of Sars-CoV: QSAR study using Density functional theory (DFT) and statistical methods

***Abdellah Ousaa[1,3], Abdelali Idrissi Taourati[2], Mohamed Chiban[1], Samir Chtita[4], Mounir Ghamali[3], Farhat Guenoun[2], Tahar Lakhlifi [3], Mohammed Bouachrine[3]**

[1] *Laboratory of Applied Chemistry and Environment, Faculty of Sciences- University ibn zohr,Agadir,Morocco.*
[2] *Laboratory of biological chemistry applied to the environment, Department of chemistry, Faculty of sciences, University Moulay Ismail, Meknes, Morocco.*
[3] *Molecular chemistry and natural substances materials laboratory, Department of chemistry, Faculty of sciences, University Moulay Ismail, Meknes, Morocco.*
[4] *Laboratory physical chemistry of materials, Faculty of sciences Ben M'Sik, Hassan II University of Casablanca,Morocco.*

**Corresponding author, Email address: abdellahousaa@gmail.com*

Received *14 Feb 2023,*
Revised *13 Mar 2023,*
Accepted *15 Mar 2023*

Citation*: Ousaa A., Taourati A. I., Chiban M., Chtita S., Ghamali M., Guenoun F., Lakhlifi T., Bouachrine M. (2023) Discovery of new inhibitors of Sars-CoV: QSAR study using Density functional theory (DFT) and statistical methods, J. Mater. Environ. Sci., 14(3), 326-336.*

Abstract: In this work, we studied a series of twenty-seven heterocyclic molecules with biological activity against SARS-CoV-1, these molecules are used to treat SARS-CoV-1 mean protease (3CLpropro or Mpro). In this work, the activity was studied by the quantitative structure-activity relationship (QSAR) to explore the important structural requirements essential to design potent SARS-CoV-1 virus inhibitors. Density functional theory (DFT) calculations with B3LYP hybrid functional employing the 6-31G (d) basis set a reused to calculate quantum chemical descriptors using Gaussian 03W software. The other topological descriptors have been calculated using MarvinSketch and ChemSketch softwares. The data set was randomly divided into learning and test sets comprising 22 and 5 compounds respectively. The multiple linear regression (MLR) model were validated internally as well as externally along with cross validation method according to the OECD principles for QSAR model validation and the Golbraikh and Tropsha's criteria of models acceptance. The best model selected with higher R^2, R^2_{test} and Q^2_{cv} values (R^2 = 0.824, R^2adj = 0.783, MSE = 0.098, R^2_{test}= 0.649, Q^2_{cv} = 0.745). Based on the established QSAR model, we proposed new molecules with very good anti-SARS-CoV-1 activity.

Keywords: *QSAR; RLM;* Heterocyclic*; Coronavirus;* SARS-CoV-1; Domain of applicability

1. Introduction

Since the death of a large number of people approximately 800 of the 8000-case recorded around around the world due to the epidemic in 2003 caused by the SARS-cov-1, boh medicine and veterinaty medicine know full well coronavirus danger (Masters *et al.*, 2006; Touzani *et al.*, 2020, *OWH, 2003*).

The virus demonstrated a great capable capacity for mutations generating new more dangerous strains with imposed the need for a control strategy.

Critical biological event that concerns SARS-CoV replication focused on (SARS-CoV 3CLpro) recognizes as very important for the design of novel anti-SARS inhibitors and the development of new anti-SARS drugs (Poutanen *et al.*,2003). The difference between SARS-CoV-2 and MERS-CoV as well as SARS-CoV has been well demonstrated; in fact, studies have shown that the nucleotide identity is up to 80% and the nucleotide similarity is up to 89.10% with the SARS-CoV genes. The similarity of the main protease of SARS-CoV3CLpro and SARS-CoV-2 represents a potential target for the screening of anti-coronaviruses inhibitors (Masters *et al.*, 2006; Unoh *et al.*, 2022). Over the whole sequence a large identity is distributed which is emanating from a strong similarity. In all probability the two proteins would have the same structure, function and would be homologous. Based on this principle, we can employ inhibitors that have already been used against the SARS-CoV 3CLpro as SARS-CoV-2 main protease attackers.

The pharmaceutical industries are developing new techniques to save time and money during the synthesis of drugs. Predictions on the biological activity of compounds are ensured by powerful computational Models, using structural qualities of the power of this equipment results in the design of extremely active molecules. According to the research of the QSAR, modeling of biological activities in nature and synthetic substances has been successfully implemented (Holmes, 2003).

27 heterocyclic derivatives substituted against SARS-Cov-1 were are collected and constructed with QSAR models to better understand the activity of chemical and biological interaction towards the virus and to orient the research for drugs towards a new path proposed against SARS-CoV-2.

The established MLR model provides a fairly precise value, similar to the real experimental value, but it remains a challenge to define the model's correct statistical properties. What's important about this work is that we used quantum chemical descriptors to describe the electronic properties of molecules using functional density theory (DFT), which improves the accuracy of the results and leads to more reliable QSAR.The proposed MLR model was used to design new molecules that could have more potential activity than the existing one (Leng *et al.*, 2003, Rota *et al.*, 2003).

2. Material and methods

2. 1. Data sources

In this work, we have chosen 27 heterocyclic molecules with biological activity anti-SARS-CoV reported in the literature (Marra et *al.*, 2003). The activity values IC_{50} (µM) which has been converted to P_{IC50} values (i.e. pIC_{50} is the negative logarithm of IC_{50} ($\boldsymbol{P_{IC50}}$=-$\log_{10}(IC_{50})$). The Table 1 shows the studied compounds and experimental activities corresponding (pIC_{50}).

Table 1: Molecular structures and observed activity values of studied compounds

N°	Molecular structures	IC50 (µM)	N°	Molecular structures	IC50 (µM)
1	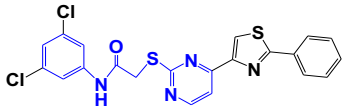	3	**15**	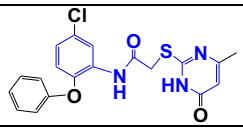	400
2*	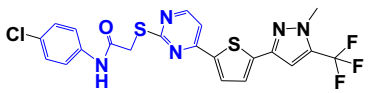	10	**16**	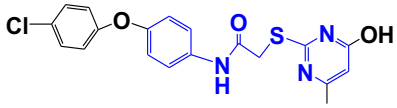	200
3	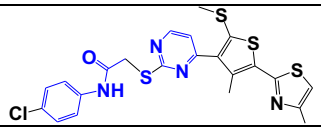	11	**17***	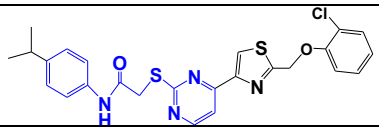	200

4	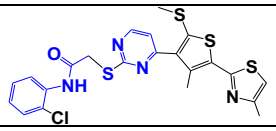	12	**18**	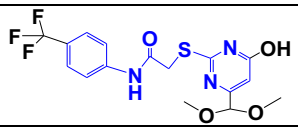	200
5	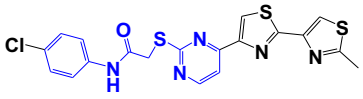	14	**19**	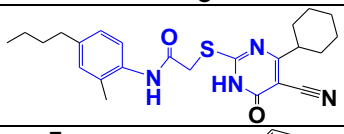	200
6	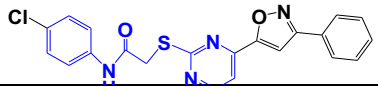	15	**20**	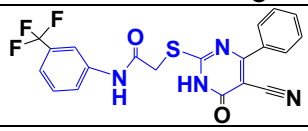	200
7	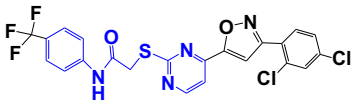	15	**21***	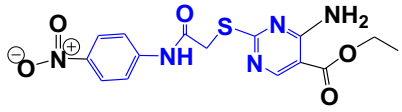	250
8	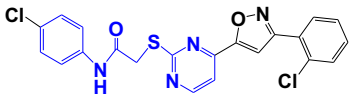	15	**22**	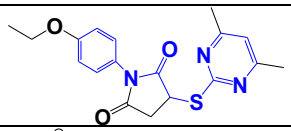	300
9*	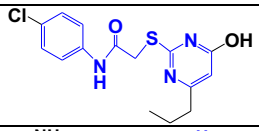	30	**23**	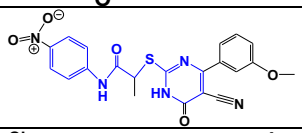	300
10	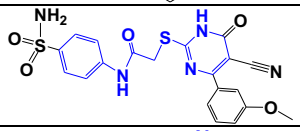	40	**24**	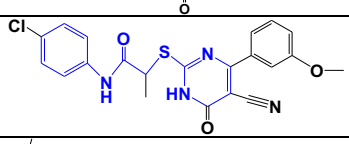	300
11	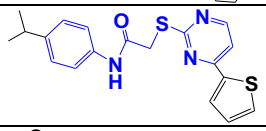	40	**25**	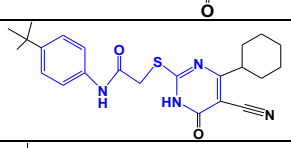	350
12	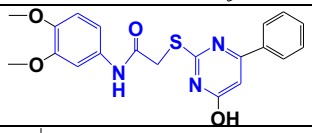	45	**26**	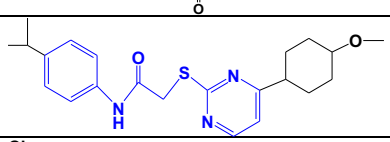	400
13*	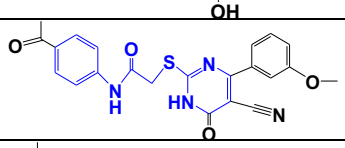	60	**27**	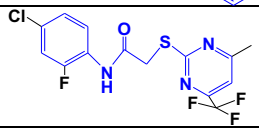	500
14	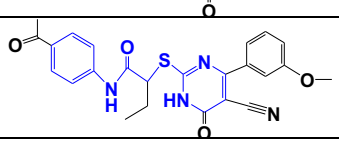	60	* test set		

2. 2. Computational methods

2. 2.1. Molecular descriptors

Several molecular descriptors can now be employed in QSAR research. They are then utilized to forecast the activity of the chemicals being researched after they have been calculated.

On the one hand, we calculated quantum descriptors using Gaussian 03W software (Snijder *et al.*, 2003). A 6-31G (d) based DFT approach was used to optimize the geometries of the 27 molecules. Then, many structural descriptors related to the results of quantum computation select in order: total-energy (E_T), dipole-moment (μ), lowest-unoccupied-molecular-orbital-energy (E_{LUMO}), highest-occupied-molecular-orbital-energy (E_{HOMO}), difference in absolute-value (ΔE), absolute-reactivity-index (ω), electronegativity (χ) and absolute-hardness (η) (Thiel *et al.*, 2003).

η, χ and ω were determined by the following equations:

$$E_{Gap} = E_{HOMO} - E_{LUMO} \; ; \; \eta = \frac{E_{HOMO} - E_{LUMO}}{2} \; ; \; \chi = \frac{E_{HOMO} + E_{LUMO}}{2} \; ; \quad \omega = \frac{\chi^2}{2\eta}$$

(Equation 1)

Also, The topological characteristics Molar-Volume (MV), Molar-Refractivity (MR), Density (d), Parachor (Pc), Polarisability (P), Refractive Index (n), and Surface Tension (**Γ**) are also calculated using the ACD/ChemSketch program (*Anand K and al.*, 2003) . The logarithm of the octanol/water partition coefficient of the test compound in its protonated state (log P), number of atoms (NA), Acceptor-count (Ac), Donor-count (Dc), Donor-sites (Ds), Acceptor-sites (Ac), Van der Waals-volume (Vwv), Dreiding energy (De), and Percentage of Composition are also computed using the MarvinSketch program (C percent ; H percent ; N percent ; O percent ; F percent ; Cl percent ; S percent).

2.2.2. Statistical analysis

To investigate the correlation between chemical descriptors, we used the Principal-Component-Analysis (PCA) method (Larif *et al.*, 2017), and the multiple linear regression (MLR) analysis with descendent collection and elimination of variables was used to create the model of structure-activity relationship. A mathematical method limits the difference between actual and predicted values. We used the program XLSTAT in the two statistical methods studies (XLSTAT Company, 2014, Taourati *et al.*, 2019).

2. 2.3. Validation of QSAR models

The approach of external internal validation was employed to validate the internal stability and predictive potential of the constructed QSAR model. At the internal validation level, the Leave-One-Out Cross Validation (LOOCV) was used; a good Q^2_{cv} reveals a QSAR model's great robustness and excellent internal predictive potential. The models developed by Globarikh and Tropsha (Golbraikh *et al.*, 2002) benefited from statistical external validation.

3. Results and discussion

3. 1. Principal component analysis

We used the Principal-Component-Analysis (PCA) method (Belhassan *et al.*, 2019) to determine the link between the various descriptors. To reduce the redundancy in our data, strongly correlated descriptors were eliminated. The following **Table 2** shows the descriptors no correlate with each, other after using the PCA method.

Table 2: Values of obtained descriptors of the studied compounds

N°	PIC50	EHOMO	ELUMO	ET	μ	log *P*	Γ	n	P	D	Dc
1	5.523	-5.484	-2.689	-76751.723	5.740	6.270	82.200	1.725	48.800	1.520	1
2	5.000	-4.821	-1.286	-73884.561	3.662	5.630	52.400	1.679	50.080	1.520	1
3	4.959	-5.200	-2.125	-87021.720	5.239	6.490	80.200	1.719	54.820	1.480	1
4	4.921	-5.200	-2.125	-87021.720	5.230	6.490	80.200	1.719	54.820	1.480	1
5	4.854	-5.529	-2.079	-74479.686	6.437	4.830	88.800	1.729	47.110	1.540	1
6	4.824	-5.643	-2.934	-55449.131	5.869	4.910	78.200	1.700	44.640	1.450	1
7	4.824	-5.739	-3.019	-77133.433	3.135	6.390	70.800	1.656	48.530	1.570	1

N°	PIC50	EHOMO	ELUMO	ET	μ	log *P*	Γ	n	P	D	Dc
8	4.824	-5.756	-2.853	-67959.090	6.944	5.520	80.000	1.705	46.560	1.510	1
9	4.523	-5.697	-1.370	-47753.232	4.306	4.130	69.700	1.643	35.020	1.380	2
10	4.398	-6.374	-3.378	-60352.019	8.189	1.020	66.500	1.701	47.780	1.510	3
11	4.398	-5.292	-1.142	-48215.728	4.690	5.010	63.800	1.654	41.550	1.290	1
12	4.347	-5.533	-1.547	-44556.385	5.972	3.970	72.800	1.668	42.440	1.380	2
13	4.222	-6.259	-3.281	-48105.114	5.020	1.980	54.200	1.656	47.070	1.340	2
14	4.222	-6.184	-3.232	-50245.524	8.777	3.070	50.900	1.641	50.650	1.300	2
15	3.398	-6.124	-2.511	-42509.691	6.061	4.480	49.200	1.638	42.320	1.280	2
16	3.699	-5.652	-1.364	-53949.464	4.394	4.480	76.600	1.689	41.830	1.450	2
17	3.699	-5.125	-1.861	-64209.219	8.630	6.520	70.900	1.672	54.910	1.380	1
18	3.699	-5.932	-1.768	-48511.182	1.964	3.440	59.300	1.578	36.450	1.450	2
19	3.699	-4.361	-2.803	-46282.056	8.085	5.600	48.800	1.634	49.840	1.240	2
20	3.699	-6.314	-3.316	-50006.886	8.770	3.450	49.800	1.360	42.730	1.420	2
21	3.602	-6.427	-3.405	-44296.217	6.379	-2.090	82.100	1.658	37.060	1.480	4
22	3.523	-6.002	-1.925	-40435.737	2.968	2.200	65.500	1.635	38.010	1.330	0
23	3.523	-6.358	-3.619	-49516.521	7.969	-2.920	63.600	1.689	45.400	1.450	4
24	3.523	-6.251	-3.248	-54413.099	6.658	3.750	55.300	1.677	44.430	1.380	2
25	3.456	-4.435	-2.916	-50105.342	7.430	4.120	49.800	1.360	42.730	1.440	2
26	3.398	-5.455	-1.491	-42602.099	6.246	5.080	59.600	1.631	44.810	1.240	1
27	3.301	-5.748	-1.791	-55440.419	6.706	4.100	54.100	1.574	32.760	1.510	1

3. 2. Multiple linear regressions (MLR)

We employed the MLR method to find a linear relationship between the studied activity and the descriptors that did not correlate with each other. This is why we divided the database into two series: 22 training compounds used to create the model and 5 test compounds used to measure the model's predictive power. After several random attempts, the best model obtained is that defined by the four descriptors, which are as follows: the energy ($\mathbf{E_{LUMO}}$) the partition-coefficient (**log *P***), the surface Tension (γ) and the Polarisability (P). The resulting equation is:

$$pIC_{50} = -0.283 - 0.247 \times E_{LUMO} + 0.099 \times \log P + 0.037 \times \gamma + 0.021 \times P \quad \text{(Equation 2)}$$

$$R^{2} = 0.824\ R^{2}_{adj} = 0.783;\ Q^{2}_{cv} = 0.745;\ MSE = 0.098;\ R^{2}_{test} = 0.649$$

The statistical parameters result of model are:

The value of determination-coefficient $\mathbf{R^2}$ close to 1, while the predicted and observed values are correlated, the value of the determination coefficient of adjustment $\mathbf{R^2_{adj}}$ is close to the $\mathbf{R^2}$, indicating that the amount of descriptors in the models is not excessive, indicating that the models are not over-fitted (*Taourati AI and al.*, 2019) [13]. The mean-squared-error (MSE) value is low.

We used the cross validation method to ensure the internal stability of the model(*Ousaa A and al.*, 2018) [16]. The high value ($\mathbf{R^2_{cv}}$**>0.5**) is enough for qualifying the model. The tall value of external validation $\mathbf{R^2_{test}}$ confirms the reliability of the mode

The VIF values are listed in **Table 3**, the VIF values of four descriptors are smaller than 4 indicating that there is no multi-collinearity among the selected descriptors, and the resulting model has good stability.

Table 3: VIF and t-test-value of descriptors in MLR model

	ELUMO	**log *P***	**Γ**	**P**
t-test-value	-2. 108	**2.625**	**5.782**	1.384
VIF	1.825	1.706	1.303	1.793

- The **t-test** values, which are also presented in **Table 3**, are another statistical measure that can be used to determine the impact of each descriptor on the examined activity of the molecules.

As a result, the following are the three key descriptors that influence the activity:

- The most essential aspect in determining the speared of a medication and its penetrability is **Surface Tension γ** (the ibility of molecules to permeate the protein surface) (Gramatica, 2007). According to the t-test values, this descriptor has the most influence on this activity; because this descriptor has a positive association, we must enhance the surface tension of molecules if we wish to boost activity.
- The **log *P*** generally replicates the lipophilicity of organic compounds, which appears to be a reasonable description of the organic compounds' transit through membranes. Because the partition coefficient in the model has a positive correlation, the activity can be raised as the lipophilicity of the examined molecules increases.
- The electro-acceptorproperty (electrophilicity) of the molecule is represented by the energy $\mathbf{E_{LUMO}}$ descriptor. The LUMO energy of a molecule determines how easy it is for it to receive electrons. Low-LUMO-energy molecules are better at accepting electrons than high-LUMO-energy molecules (Ahamed *et al.*, 2019).

Table 4: Descriptors values of the new designed compound and their anti-coronavirus activity (IC50) calculated by MLR equation

N	**Structures**	**ELUMO**	**log *P***	**ϒ**	**P**	**IC50 (µM)**
1	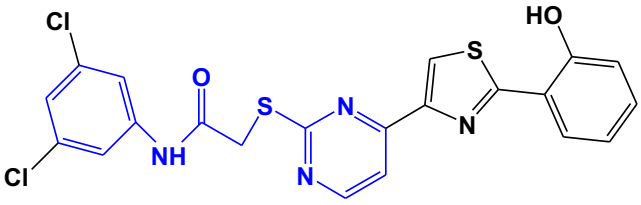	-2. 537	5. 96	91. 3	49. 41	4. 7
2	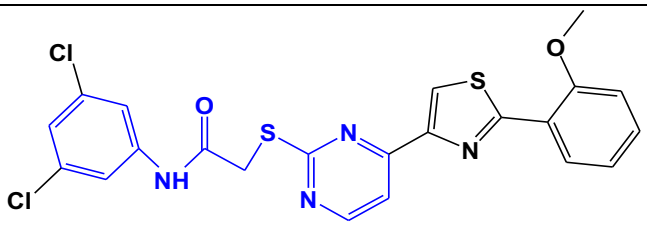	-2. 507	6. 11	80	51. 32	10. 3

3	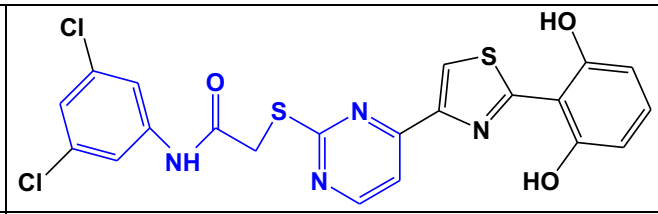	-2. 264	5. 66	101. 5	50. 01	2. 4
4	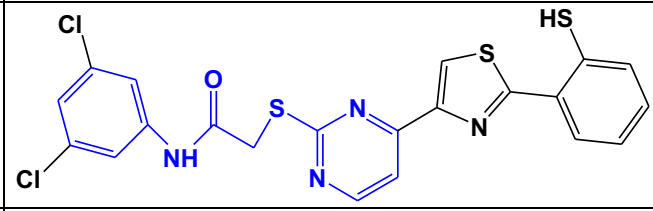	-2. 759	6. 36	85. 7	51. 91	5. 3
5	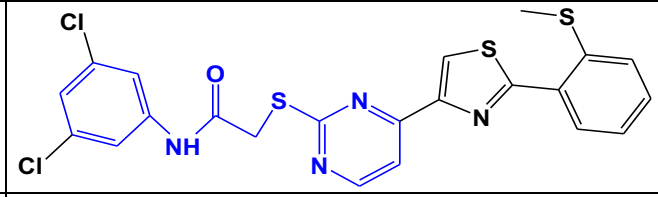	-2. 654	6. 9	82. 8	53. 81	5. 5
6	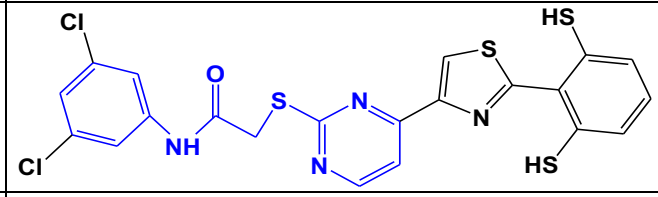	-2. 682	6. 45	89	55. 02	3. 5
7	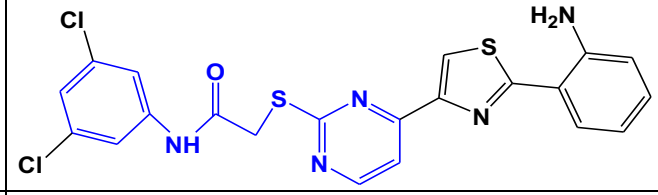	-2. 438	5. 44	88. 9	50. 23	6. 5
8	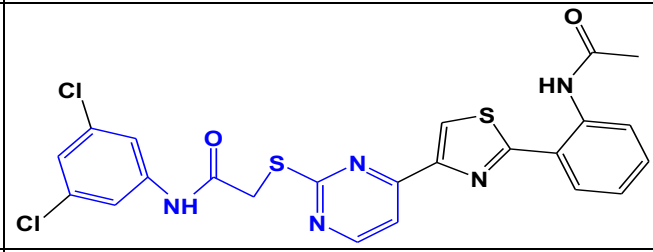	-2. 720	5. 51	83. 2	53. 96	7. 3
9	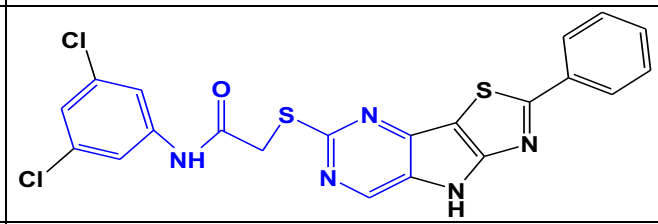	-1. 970	5. 83	96. 7	50. 52	3. 7
10	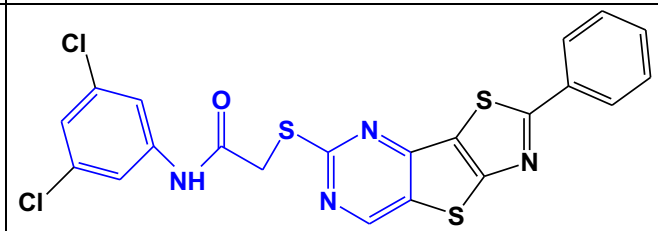	-2. 008	6. 68	93. 1	52. 19	3. 6
11	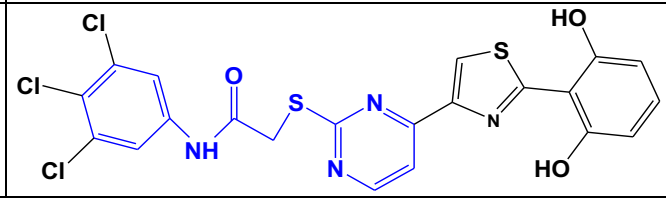	-2. 295	6. 27	102. 7	51. 92	1. 6

12	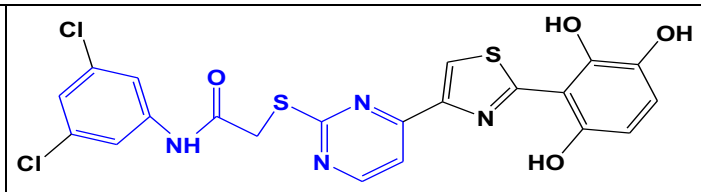	-2. 284	5. 36	112. 8	50. 62	1. 01
13	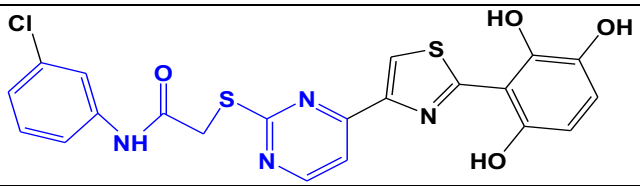	-2. 293	4. 75	111. 8	48. 7	1. 4
14	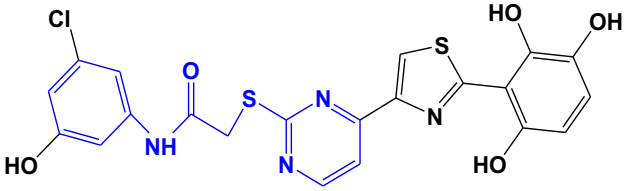	-2. 229	4. 45	124. 3	49. 31	0. 5
15	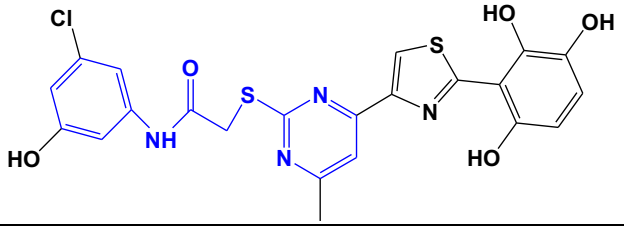	-2. 154	4. 58	117. 9	51. 14	0. 8
16	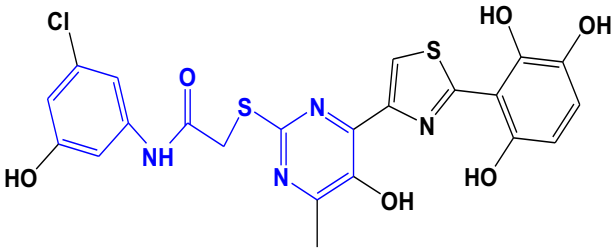	-2. 027	4. 28	130. 7	51. 75	0. 332
17	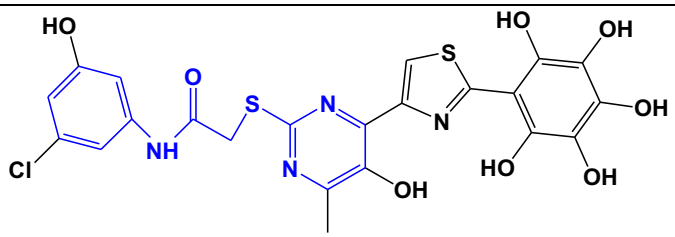	-2.010	4.03	148.4	53.83	0.080
18	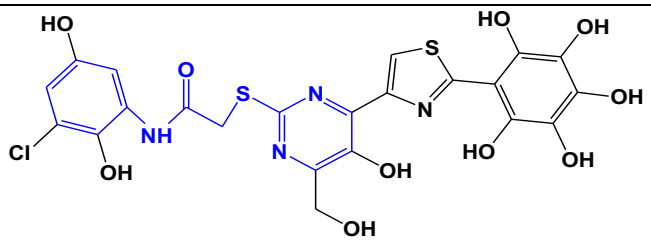	-2.003	2.55	197.30	54.18	0.002
19	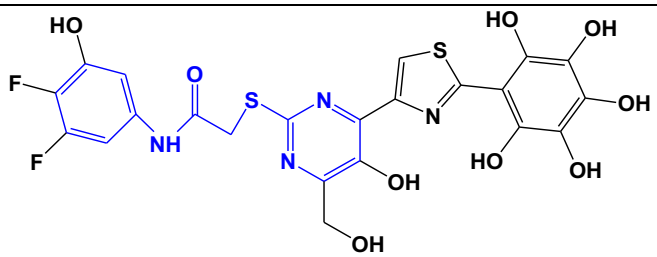	-2.006	2.53	168.00	51.75	0.026

20	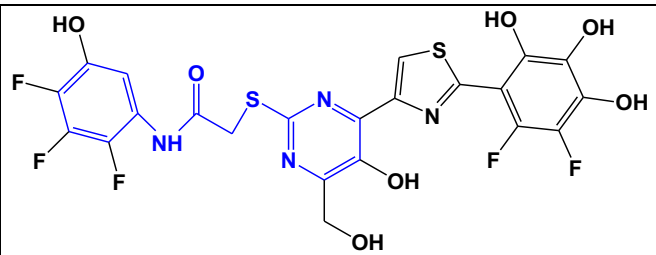	-2.085	3.75	124.80	50.67	0.631
21	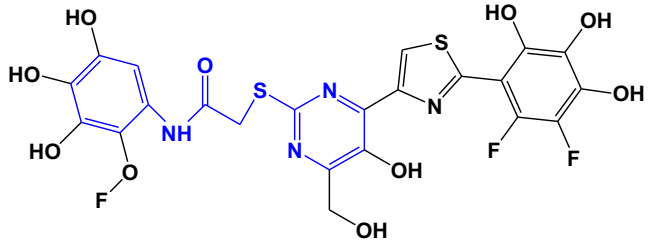	-2.047	2.63	162.1	52.48	0.038
22	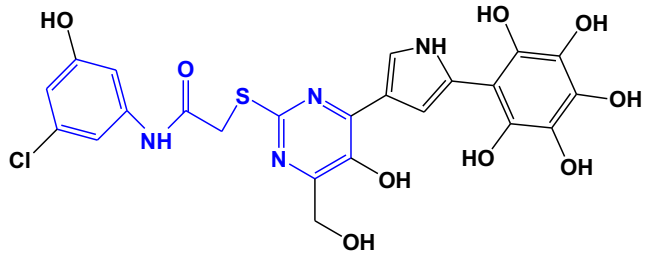	-1.539	2.13	192.3	53.38	0.005

3.3. Domain of applicability

To estimate the reliability of any QSAR model and its ability to predict new compounds, the domain of applicability must be essentially defined (Ousaa A and *al.*, 2018). The predicted compounds that fall within this domain may be considered as reliable. The applicability domains were discussed with the Williams graphs in figure 1 of the MLR model respectively, which the standardized residuals and the leverage values (hi) are plotted.

It is based on the calculation of the leverage h_i for each molecule, for which QSAR model is used to predict its activity:

$$h_i = x_i\,(X^T\,X)^{-1}\,x_i^T \qquad i = 1\ldots n \qquad \textbf{(Equation 3)}$$

Where x_i is the row vector of the descriptors of compound i and X is the variable matrix deduced from the training set variable values. The index T refers to the matrix/vector transposed. The critical leverage h^* is generally fixed at (3k+1)/N, where N is the number of training molecules, and k is the number of model descriptors. If the leverage value h of molecule is higher than the critical value (h^*) i.e., $h > h^*$, the prediction of the compound can be considered as not reliable.

As shown in the Williams graphs in **figure 1** of the MLR models plot the majority of the compounds in the dataset are in this area, except except compounds 3 and 4 in test set exceeds the threshold and it is considered as an outlier compound, also, compound 15 in the training set is consid-ered as an outlier because it exceeds the crucial hat value (h* = 0.6). Therefore, the predicted activity by the developed MLR model is reliable.

3.4. Design of new compounds

A new method of a research on anti-coronaviruses drugs many results from additional knowledge from derivatives according to table 1. There is a good chance for fining new remedies against SARS-CoV1 and SARS-CoV-2 since they are part of the same family, through developing with the previous ones.

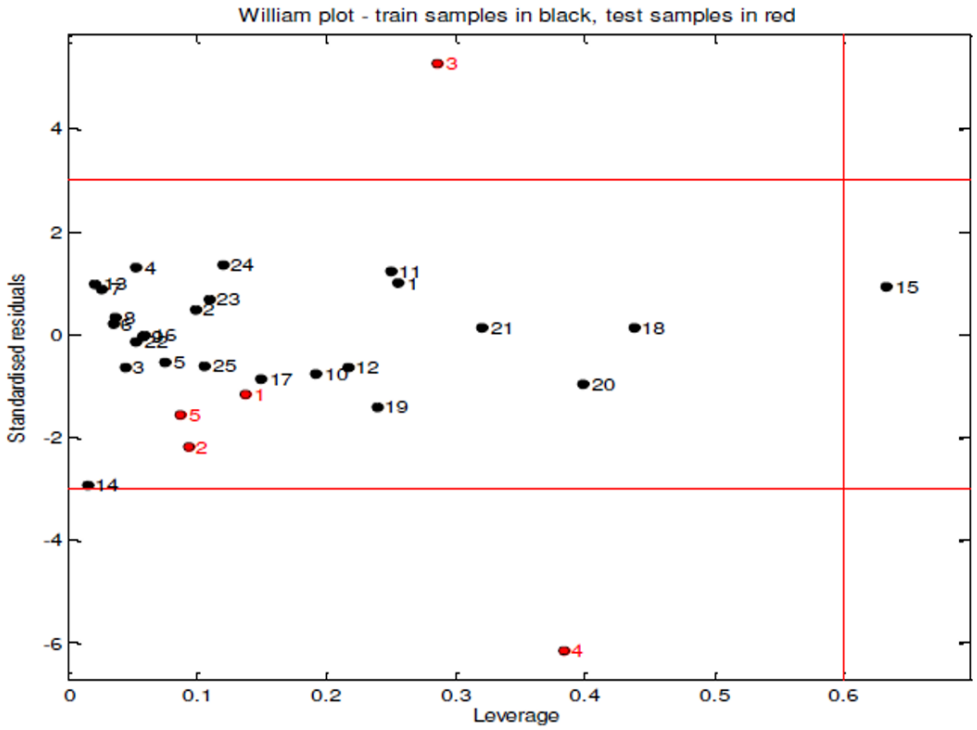

Figure 1: Williams plot for the MLR model (with $h^* = 0.6$ and residual limits = ±3σ).

Using the lowest Ic50 value, a compound's structure was adjusted according to the same method. Table 4 displays the developed compounds' structures, as well as the theoretical IC50 values predicted by the MLR model using the same approaches.

Conclusion

The multiple linear regressions (MLR) approaches were used as a linear feature QSAR method to interpret the relationship between coronavirus inhibitory activity for 27 derivatives acting as anti-coronavirus drugs and their structural descriptors obtained by density functional theory calculation with Becke's three-parameter hybrid method and the Lee-Yang-Parr B3LYP functional using the 6–31G (d) basis set.

Such as the accuracy and predictability of the proposed models were checked based on the domain of applicability (AD) of the MLR model.

According to the findings, heterocyclic compounds with the following structural characteristic may have strong anti-coronavirus activity. The most noteworthy outcomes of this research, according to the proposed model, are that we have built and suggested some novel compounds with potentially great activity. These findings urge theoretical pharmacologists to collaborate with academic and industry pharmacologists.

References

Ahamed T.S., Rajan V.K., Muraleedharan K. (2019). QSAR modeling of benzoquinone derivatives as 5-lipoxygenase inhibitors. *Food Sci Hum Wellness*. 8, 53–62. Doi: 10.1016/j.fshw.2019.02.001.

Anand K., Ziebuhr J., Wadhwani P., *et al.* (2003). Coronavirus main proteinase (3CLpro) structure: basis for design of anti-SARS drugs. *Science,* 300, 1763–1767. Doi: 10.1126/science.1085658

Belhassan A., Chtita S., Lakhlifi T., Bouachrine M. (2019). QSPR Study of the Retention/Release Property of Odorant Molecules in Water, Dairy and Pectin gels. *Mater. Today Proc.* 13, 621–629. https://doi.org/10.1016/j.matpr.2019.04.021

Belhassan A., Chtita S., Lakhlifi T., Bouachrine M. (2018). QSRR Study of Linear Retention Indices for Volatile Compounds using Statistical Methods. Chem Sci. 7, 558–575. Doi: 10.5772/intechopen.89576
Golbraikh A, Tropsha A. (2002). Beware of q2! *J. Mol. Graph. Model.* 20, 269–276. https://doi.org/10.1016/S1093-3263(01)00123-1
Gramatica .P. (2007). Principles of QSAR models validation: internal and external. *QSAR Comb Sci.* 26, 694–701. https://doi.org/10.1002/qsar.200610151
Holmes K.V. (2003). SARS-associated coronavirus. *N. Engl. J. Med.* 348, 1948–1951. Doi: 10.1056/NEJMp030078
Larif M., Adad A., Hmammouchi R., *et al.* (2017). Biological activities of triazine derivatives. Combining DFT and QSAR results. *Arab. J. Chem.* 10, S946–S955. https://doi.org/10.1016/j.arabjc.2012.12.033
Leng Q., Bentwich Z. (2003). A novel coronavirus and SARS. *N. Engl. J. Med.* 349, 709 – 709. Doi:10.1056/NEJMc031427
Marra M.A., Jones S.J., Astell C.R., et al. (2003). The genome sequence of the SARS-associated coronavirus. *Science.* 300,1399–1404. Doi: 10.1126/science.1085953
Masters P.S. (2006). The molecular biology of coronaviruses. *Adv. Virus Res.* 66, 193–292. Doi: 10.1016/S0065-3527(06)66005-3
Ousaa A., Elidrissi B.,Ghamali M., Chtita S., Aouidate A., Bouachrine M. and Lakhlifi T., (2018). QSAR study of (5-nitroheteroaryl-1,3,4-thiadiazole-2-yl) piperazinyl derivatives to predict new similar compounds as antileishmanial agents. *Advances in Physical Chemistry*. https://doi.org/10.1155/2018/2569129
Organization W.H. (2003). Summary of probable SARS cases with onset of illness from 1 November 2002 to 31 July 2003. Doi: 10.1046/j.1440-1843.2003.00516.x
Poutanen S.M., Low D.E., Henry B., et al. (2003). Identification of severe acute respiratory syndrome in Canada. *N. Engl. J. Med*. 348, 1995–2005 Doi: 10.1056/NEJMoa030634Rota P.A., Oberste M.S., Monroe S.S., et al. (2003). Characterization of a novel coronavirus associated with severe acute respiratory syndrome. *Science.* 300, 1394–1399. Doi: 10.1126/science.1085952
Snijder E.J., Bredenbeek P.J., Dobbe J.C., et al. (2003). Unique and conserved features of genome and proteome of SARS-coronavirus, an early split-off from the coronavirus group 2 lineage. *J. Mol. Biol*. 331, 991–1004. Doi: 10.1016/s0022-2836(03)00865-9
Thiel V., Ivanov K.A., Putics A., et al. (2003). Mechanisms and enzymes involved in SARS coronavirus genome expression. *J. Gen. Virol.* 84, 2305–2315. Doi: 10.1099/vir.0.19424-0
Taourati A.I., Zaki H., Ghamali M., et al. (2019). Anti-Proliferative Activity of Heterocyclic Compounds Based on Indole. QSAR study. 12.
Touzani R., Hammouti B., El Malki F., Benhadda T. (2020). Coronavirus, covid19, covid-19 and sars-cov-2: A global pandemic, a short review, *Journal of Materials and Environmental* Science 11 (5), 736
Unoh Y., Uehara S., Nakahara K., Nobori H., Yamatsu Y., Yamamoto S., Maruyama Y., Taoda Y., Kasamatsu K., Suto T., Kouki K., Nakahashi A., Kawashima S., Sanaki T., Toba S., Uemura K., Mizutare T., Ando S., Sasaki M., Orba Y., Sawa H., Sato A., Sato T., Kato T., and Tachibana Y. (2022). *Journal of Medicinal Chemistry*, 65(9), 6499-6512 DOI: 10.1021/acs.jmedchem.2c00117
XLSTAT Company. (2014). XLSTAT 2014 software.